Evolution of a Vacuum Shell in the Friedman-Schwarzschild World

V. I. Dokuchaev*
Institute for Nuclear Research of the Russian Academy of Sciences, 60-letiya Oktyabrya pr. 7a, Moscow, 117312 Russia

S. V. Chernov†
Lebedev Physical Institute of the Russian Academy of Sciences, Leninskii pr. 53, Moscow, 119991 Russia and Institute for Nuclear Research of the Russian Academy of Sciences, 60-letiya Oktyabrya pr. 7a, Moscow, 117312 Russia

(Dated: August 29, 2008)

The method of an effective potential is used to investigate the possible types of evolution of vacuum shells in the Friedman- Schwarzschild world. Such shells are assumed to emerge during phase transitions in the early Universe. The possible global geometries are constructed for the Friedman- Schwarzschild worlds. Approximate solutions to the equation of motion of a vacuum shell have been found. The conditions under which the end result of the evolution of the vacuum shells under consideration is the formation of black holes and wormholes with baby universes inside have been found. The interior of this world can be a closed, flat, or open Friedman universe.

PACS numbers: 04.20.-q, 04.70.-s, 98.80.-k

I. INTRODUCTION

Phase transitions in the early Universe occur with the formation of vacuum bubbles of a new phase. During the expansion and mutual intersection of new-phase bubbles, old-phase bubbles completely surrounded by the new phase can also be formed [1, 2, 3, 4, 5, 6, 7]. Investigating the evolution of such bubbles and their subsequent fate is of interest in connection with the problems of primordial black holes. The evolution of vacuum bubbles was considered in many papers mainly under the assumption of a de Sitter metric for the bubble interior. The region that separates the bubble interior and exterior is a domain wall. The shin-shell formalism suggested by Israel [8] and subsequently developed in detail by Berezin, Kuzmin, and Tkachev [9], as applied to cosmological problems, is commonly used to describe the latter. Various special cases of this problem were considered in many papers on cosmological phase transitions (see, e.g., the early papers [3, 4, 5, 7, 10, 11, 12, 13]). The end result of the evolution of vacuum bubbles can be the formation of primordial black holes and various types of wormholes with baby universes inside [9, 10, 14, 15, 16, 17, 18, 19, 20, 21, 22, 23, 24, 25]. The evolution of vacuum bubbles in the Schwarzschild-de Sitter world was investigated in [9, 24, 26, 27]. The dynamics of a bubble in the Friedman-Schwarzschild world was investigated in [10, 11] but without including the surface tension of the bubble (shell) wall. In this paper, we analyze the full dynamics of a vacuum shell in the Friedman- Schwarzschild world in the thin-wall approximation by taking into account the surface energy density of the shell. Such a configuration can result from the production of particles during the vacuum decay inside the bubble by analogy with the final stage of inflation (see also [28]). As a result of our analysis, we found all of the possible types of evolution of vacuum shells in the Friedman-Schwarzschild world and constructed the corresponding global geometries. We also found approximate asymptotic solutions to the equation of motion of vacuum shells in the Friedman- Schwarzschild world.

II. A SHELL IN THE FRIEDMAN-SCHWARZSCHILD WORLD

Let us consider a spherically symmetric shell whose interior (far from the boundary) is described by the Friedman metric

$$ds^2 = dt_{\rm in}^2 - a^2(t_{\rm in})\left[\frac{dq^2}{1-kq^2} + q^2 d\Omega^2\right], \qquad (1)$$

where $t_{\rm in}$ is the time of an observer in the Friedman world, $a = a(t_{\rm in})$ is the scale factor, q is the inner radial coordinate, $d\Omega$ is an element of the solid angle, $k = 1$, $k = 0$, and $k = -1$ for closed, flat, and open worlds, respectively. The exterior of the shell is described by the Schwarzschild metric

$$ds^2 = \left(1 - \frac{2m}{r}\right) dt_{\rm out}^2 - \left(1 - \frac{2m}{r}\right)^{-1} dr^2 - r^2 d\Omega^2, \quad (2)$$

where m is the total outer mass of the shell and r is the outer radial coordinate. In what follows, the subscripts "in" and "out" pertain to the inner Friedman and outer Schwarzschild worlds, respectively. The metric of the transition region is modelled in the form of a thin shell Σ:

$$ds^2|_\Sigma = d\tau^2 - \rho^2(\tau) d\Omega^2, \qquad (3)$$

*Electronic address: dokuchaev@ms2.inr.ac.ru
†Electronic address: chernov@td.lpi.ru

where τ is the proper time of an observer on the shell and $\rho = \rho(\tau)$ is the shell radius. The inner and outer metrics are joined on the shell using the thin-shell method [8] to give the equations of motion of the shell [9]

$$4\pi S_0^0 = [K_2^2], \quad \frac{dS_0^0}{d\tau} + 2(S_0^0 - S_2^2)\frac{\dot{\rho}}{\rho} + [T_0^n] = 0, \quad (4)$$

where S_α^β is the surface energy density tensor on the shell, K_α^β is the external curvature tensor, T_α^β is the fluid energy-momentum tensor, and $[A] = A_{out} - A_{in}$. For a vacuum shell, $S_0^0 = S_2^2 = S = const$. Let us first consider the interior of our bubble. The Friedman equations are

$$\frac{\dot{a}^2 + k}{a^2} = \frac{8\pi}{3}\varepsilon, \qquad \frac{\ddot{a}}{a} = -\frac{4\pi}{3}(\varepsilon + 3P), \quad (5)$$

where the dot denotes differentiation with respect to the time t_{in}, ε is the energy density, and P is the pressure. We will make the classification for an arbitrary equation of state, but we will always keep in mind a linear equation of state, where $P = \alpha\varepsilon$ and $\alpha = const \neq -1$ (for the classification of solutions in the case of $\alpha = -1$ corresponding to the de Sitter vacuum metric, see [26, 27]). For a linear equation of state, the solution to the Friedman equations is ($k = 0$)

$$a = At_{in}^n, \quad \varepsilon = \frac{3n^2}{8\pi t_{in}^2}, \quad (6)$$

where A is a constant and $n = 2/(3(1+\alpha))$. For the Friedman metric and using the condition for joining the Friedman metric and the shell, $\rho = aq$, Berezin et al. [9] calculated (for any k) the invariants

$$\Delta \equiv g^{\alpha\beta}\rho_{,\alpha}\rho_{,\beta} = \frac{8\pi}{3}\varepsilon\rho^2 - 1 \quad (7)$$

and the external curvature tensor component (since the problem is spherically symmetric, we will need only one component)

$$K_2^2 = -\frac{\sigma}{\rho}\sqrt{\left(\frac{d\rho}{d\tau}\right)^2 + 1 - \frac{8\pi}{3}\varepsilon\rho^2}, \quad (8)$$

where $\sigma = \pm 1$; $\sigma = 1$ if the radius of the two-dimensional sphere increases in the direction of the outward normal and $\sigma = -1$ in the opposite case. In turn, depending on the sign of the invariant Δ, the shell moves either in the space-time region R or in T [29]. The boundary that separates the space-time regions R and T for the Friedman metric is located at the radius

$$\rho_\Delta = \sqrt{\frac{3}{8\pi\varepsilon}}, \quad (9)$$

which is the root of the equation $\Delta(\rho) = 0$. For the outer Schwarzschild metric, the external curvature tensor component K_2^2 is

$$K_2^2 = -\frac{\sigma}{\rho}\sqrt{\left(\frac{d\rho}{d\tau}\right)^2 + 1 - \frac{2m}{\rho}}, \quad (10)$$

and the radius at which Δ changes its sign coincides with the radius of the event horizon $r_h = 2m$. As a result, the main equation of motion of the shell (4) that arises as a condition for joining the outer and inner metrics can be written for any k as [9]

$$4\pi S = \frac{\sigma_{\text{in}}}{\rho}\sqrt{\left(\frac{d\rho}{d\tau}\right)^2 + 1 - \frac{8\pi}{3}\varepsilon\rho^2} - \frac{\sigma_{\text{out}}}{\rho}\sqrt{\left(\frac{d\rho}{d\tau}\right)^2 + 1 - \frac{2m}{\rho}}. \quad (11)$$

In this equation, the radius ρ depends on the proper time τ of an observer on the shell and the energy density ε depends on the time t_{in} for an observer inside the shell in the Friedman world. Therefore, the equation of motion should be supplemented with another equation obtained when the inner Friedman metric and the metric on the shell are joined:

$$dt_{in}^2 - a^2 dq^2 = d\tau^2. \quad (12)$$

In the Eq. (11), the shell radius ρ may be considered as a function of the time t_{in} (below, we omit the subscript to save space). More specifically, $\tau = \tau(t)$ can be expressed from Eq. (12) and substituted into Eq. (11), i. e., $\rho(\tau) = \rho(\tau(t))$. We will begin our analysis with the full classification of the solutions to the equation of motion of the shell (11) and the construction of the corresponding global geometries. Subsequently, we will find an approximate solution to the equation of motion of the shell in some special cases.

III. ANALYSIS OF THE EQUATION OF MOTION OF THE SHELL

For the subsequent analysis, it is convenient to represent the equation of motion of the shell (11) as an equation for the effective energy,

$$(d\rho/d\tau)^2/2 + U(\rho) = 0$$

(see also [26, 27]), where the effective potential is

$$U(\rho)=\frac{1}{2}\left[1-\left(2\pi S+\frac{\varepsilon}{3S}\right)^2\rho^2-\frac{m}{\rho}\left(1-\frac{\varepsilon}{6\pi S^2}\right)-\frac{m^2}{16\pi^2S^2\rho^4}\right]. \tag{13}$$

Its graph is presented in Fig. 1. Equation (13) for the effective potential $U(\rho)$ should be supplemented with the following conditions on the signs of the quantity σ present in the original equation of motion of the shell (11):

$$\sigma_{\rm in} \;=\; sign\left[m-\frac{4\pi}{3}\varepsilon\rho^3+8\pi^2S^2\rho^3\right], \tag{14}$$

$$\sigma_{\rm out} \;=\; sign\left[m-\frac{4\pi}{3}\varepsilon\rho^3-8\pi^2S^2\rho^3\right]. \tag{15}$$

It is easy to show that the second derivative of this potential with respect to the radius for any $\rho=\rho(\tau(t))$ is negative:

$$\frac{\partial^2U}{\partial\rho^2}=-\frac{1}{2}\left[\frac{2m}{\rho^3}+\frac{m^2}{\pi^2S^2\rho^6}+8\pi^2S^2+\frac{8\pi}{3}\varepsilon+\frac{\varepsilon^2}{9S^2}+\left(\frac{\varepsilon}{3S}-\frac{m}{2\pi S\rho^3}\right)^2\right]<0\,. \tag{16}$$

Thus, there are no static solutions in this problem [30]. Setting the first derivative of the potential with respect to the radius equal to zero, we find the point of maximum potential $\rho^3_{\rm max}=my_{\rm max}$, where

$$y_{\rm max}=\left[1-\frac{\varepsilon}{6\pi S^2}+\sqrt{\left(1-\frac{\varepsilon}{6\pi S^2}\right)^2+8\left(1+\frac{\varepsilon}{6\pi S^2}\right)^2}\right]\left(4\pi S+\frac{2\varepsilon}{3S}\right)^{-2}>0. \tag{17}$$

Note, that the point of maximum potential is a function of time, $\rho_{\rm max}=\rho_{\rm max}(t)$. As will be shown below, the total mass m (Schwarzschild mass) of the shell measured by an observer at spatial infinity is a convenient parameter for the classification of the possible types of its evolution. This mass with the gravitational mass defect includes the total energy of the inner Friedman world and the total energy of the shell with its surface tension energy and its kinetic energy. Substituting $\rho=\rho_{\rm max}$ into Eq. (13) for the potential, we find the first important mass parameter of the shell, $m_{\rm max}=m_0$, at which a contracting or expanding shell passes through the point of maximum potential:

$$m_0=\sqrt{y_{\rm max}}\left[1-\frac{\varepsilon}{6\pi S^2}+\frac{1}{16\pi^2S^2y_{\rm max}}+\left(2\pi S+\frac{\varepsilon}{3S}\right)^2y_{\rm max}\right]^{-3/2}>0. \tag{18}$$

The potential $U(\rho_{\rm max})<0$ for $m>m_0$ and, conversely, $U(\rho_{\rm max})>0$ for $m<m_0$. Thus, depending on the total mass m of the shell, the potential either intersects the $U=0$ axis or does not. In other words, this means that the presence or absence of a bounce point during the temporal evolution of the shell radius depends on the total mass m of the shell. It should be kept in mind that the mass parameter m_0 (and all of the mass parameters introduced below) is a function of time t, because the energy density ε depends on t in accordance with the Friedman equations (5). Therefore, at a fixed total mass m, inequalities of the form $m>m_0$ or $m<m_0$ can change with time to the opposite ones. Accordingly, the bounce point can appear and/or disappear as the

shell evolves. Note also that the energy density ε decreases with time for a linear equation of state, $P = \alpha\varepsilon$, at $\alpha > -1$ and $k = 0$. Therefore, on fairly long time scale, we have the following asymptotic for the mass parameter: $m_0(t \to \infty) = 4/(27\pi S)$ Accordingly, the inequality $U(\rho_{\max}) \lesseqgtr 0$ will hold on fairly long time scales for $m \gtreqless m_0(t \to \infty)$. Next, it follows from Eq. (14) that $\sigma_{\rm in}$ changes its sign ($\sigma_{\rm in} = 0$) at the shell radius $\rho = \rho_1$, where

$$\rho_1^3 = \frac{3}{4\pi}\,\frac{m}{\varepsilon - 6\pi S^2}, \tag{19}$$

The radius ρ_1 exists only at $\varepsilon(t,k) > 6\pi S^2$. For a linear equation of state, $t < t_1 = n/(4\pi S)$ at $k = 0$. The radius ρ_1 does not exist ($\rho_1 < 0$) at $t > t_1$. We see from these relations that on time scales $t < t_1$ there exists a radius in a flat universe at which σ_{in} changes its sign; the latter, in turn, is related to the regions R_+ (where $dr/dq > 0$) and R_- (where $dr/dq < 0$). The solution of the Friedman equations determines the time scales at which the radius ρ_1 will exist for other equations of state. Note also that a periodic function can be the solution of the Friedman equations for a closed universe. Therefore, the radius ρ_1 can appear and disappear an infinite number of times. We will assume that the radius appears only once. This is a very rough approximation that can subsequently lead to contradiction on the Carter-Penrose diagrams if this condition is disregarded. In turn, it follows from Eq. (15) that $\sigma_{\rm out}$ changes its sign ($\sigma_{\rm out} = 0$) at the shell radius $\rho = \rho_2$, where

$$\rho_2^3 = \frac{3}{4\pi}\,\frac{m}{\varepsilon + 6\pi S^2}, \tag{20}$$

The relations between ρ_1, ρ_2 and $\rho_{\max}$ follow from Eqs. (17), (19) and (20):

$$\rho_2 \;<\; \rho_{\max}; \tag{21}$$

$$\rho_1 \;>\; (\rho_2, \rho_{\max}) \quad \text{for} \quad \varepsilon > 6\pi S^2. \tag{22}$$

Substituting the radius $\rho = \rho_1$ into Eq. (13) for the potential $U(\rho)$ and solving the equation

$$U(\rho_1) \equiv \frac{1}{2}\left[1 - 2\left(\frac{4\pi}{3}\right)^{1/3}\left(\frac{m\varepsilon^{3/2}}{\varepsilon - 6\pi S^2}\right)^{2/3}\right] = 0. \tag{23}$$

we find the mass parameter $m = m_1$, where

$$m_1 = \frac{1}{4}\sqrt{\frac{3}{2\pi}}\frac{\varepsilon - 6\pi S^2}{\varepsilon^{3/2}}. \tag{24}$$

We see from this relation that $U(\rho_1) \lesseqgtr 0$ for $m \gtreqless m_1$. This parameter exists, just as ρ_1, only at $\varepsilon > 6\pi S^2$. Similarly, substituting the radius $\rho = \rho_2$ into Eq. (13) for the potential $U(\rho)$ and solving the equation

$$U(\rho_2) \equiv \frac{1}{2}\left[1 - 2\left(\frac{4\pi}{3}\right)^{1/3} m^{2/3}(\varepsilon + 6\pi S^2)^{1/3}\right] = 0, \tag{25}$$

we find another mass parameter, $m = m_2$, where

$$m_2 = \frac{1}{4}\sqrt{\frac{3}{2\pi(\varepsilon + 6\pi S^2)}}. \tag{26}$$

According to Eq. (6), the energy density in the Friedman world decreases as $\varepsilon \propto t^{-2}$ (for a linear equation of state and at $k = 0$). Therefore, the mass parameter m_2 increases with time:

$$dm_2/dt > 0, m_2(t \to \infty) \to (8\pi S)^{-1} \tag{27}$$

For $m < m_2$, the potential is always positive at the point with $\rho = \rho_2$, i. e., $U(\rho_2) > 0$. In contrast, for $m > m_2$, the potential is always negative at the point with $\rho = \rho_2$, i. e., $U(\rho_2) < 0$. In other words, the point with coordinates $(\rho_2, 0)$ lies under the graph of $U(\rho)$ for $m < m_2$ and above the graph of $U(\rho)$ for $m > m_2$. At $m = m_2$, the radius ρ_2 intersects the potential. Note also that $m_2 > m_1$. For the potential on the event horizon of the Schwarzschild metric, $\rho_h = 2m$, we find

$$U(\rho_h) = -\left[\pi S m\left(1 + \frac{\varepsilon}{6\pi S^2}\right) - \frac{1}{64\pi S m}\right]^2 \le 0. \tag{28}$$

We see that the point with coordinates $(\rho_h, 0)$ always lies either above the graph of $U(\rho)$ or touches the graph of the potential at $m = m_2$ ($U(\rho_h) = 0$). At $m = m_2$, the radius of the event horizon $\rho_h = 2m$ coincides with the radius ρ_2 at which $\sigma_{\rm out}$ changes its sign. Using Eqs. (18), (20) and (26) for m_0, ρ_2 and m_2, we find that $m_0 > m_2$ and

$$\rho_h \gtreqless \rho_2 \quad \text{for} \quad m \gtreqless m_2. \tag{29}$$

Finally, substituting the radius of the boundary between the space-time regions R and T in the Friedman world, $\rho = \rho_\Delta$ from (9), into Eq. (13) for the potential $U(\rho)$ yields

$$U(\rho_\Delta) = -\frac{1}{2\rho_\Delta}\left[2\pi S\left(1 - \frac{\varepsilon}{6\pi S^2}\right)\left(\frac{3}{8\pi\varepsilon}\right)^{3/4} + \frac{m}{4\pi S}\left(\frac{8\pi\varepsilon}{3}\right)^{3/4}\right]^2 \le 0. \tag{30}$$

We see that the point with coordinates $(\rho_\Delta, 0)$ cannot be under the graph $U(\rho)$. Only at $m = m_1$ does the point with coordinates $(\rho_\Delta, 0)$ lie on the graph of the potential and, in this case, $\rho_\Delta = \rho_1$. Accordingly, $\rho_1 \gtrless \rho_\Delta$ for $m \gtrless m_1$. Note that the radius ρ_Δ at which the regions R and T are interchanged has the same properties as the radius of the event horizon in the Schwarzschild metric, $r_h = 2m$, with respect to our potential. It can also be shown that $\rho_\Delta > \rho_{\max}$ at $m = m_{\max}$. Finally, let us introduce the last mass parameter

$$m_3 = \frac{1}{4}\sqrt{\frac{3}{2\pi\varepsilon}}, \tag{31}$$

which is the root of the equation $\rho_\Delta = \rho_h$. As a result, we will obtain the relations $\rho_h \lessgtr \rho_\Delta$ for $m \lessgtr m_3$. It can be shown that $m_3 > m_0$. For a linear equation of state, $m_3(t \to \infty) \to \infty$ at $k = 0$. We now have all of the necessary parameters to construct a full classification of the possible types of solutions to the equation of motion of the shell in the Friedman-Schwarzschild world and to find the corresponding global geometries.

IV. GLOBAL GEOMETRIES OF THE FRIEDMAN-SCHWARZSCHILD WORLD

Let us consider all of the possible types of solutions to the equation of motion of a vacuum shell in the Friedman-Schwarzschild world and then give a physical interpretation of these solutions.

A. The Case of $m > m_3$

We will begin our consideration with the case where $m > m_3$, i. e., where the shell has a large mass that exceeds all of the characteristic masses in our problem, and will sequentially consider shells with an increasingly small mass. In this case, the relations $\rho_h > \rho_\Delta$, $\rho_1 > \rho_2$ (if ρ_1 exists), $\rho_1 > \rho_\Delta$ and $\rho_h > \rho_2$ hold. The potential and the location of the characteristic radii for this case are shown in Fig. 2a. As we see from Fig. 2a, there is no bounce point for the vacuum shell in this case. Let us consider the special case where the vacuum shell initially expands. To determine the type of space-time regions R and T, it is important to know which signs σ_{in} and σ_{out} will have when the shell intersects the radii ρ_Δ and ρ_h, respectively. When the radius ρ_Δ is intersected, $\sigma_{\text{in}} = 1$ for any function $\varepsilon(t, k)$. Consequently, the shell initially moves in the region R_+. When the radius ρ_h is intersected, $\sigma_{\text{out}} = -1$ and, hence, the shell is in the region R_-. The Carter-Penrose diagram (global geometry) corresponding to this case is shown in Figs. 2b-2d (at $k = 0, -1$) for various equations of state (see also [29]). Below, we will give the Carter-Penrose diagrams only for the case where $P = \varepsilon/3$, i. e., $\alpha = 1/3$, since the corresponding diagrams for other equations of state with $\alpha = const$ are constructed in a similar way. The Carter-Penrose diagrams for a closed universe will be the same as those for an open one (see Figs. 2b-2d). For a contracting shell, the signs of σ at which the shell intersects the radii ρ_h and ρ_Δ will remain the same. The corresponding Carter-Penrose diagram for a closed geometry is shown in Fig. 2e. Additional peculiarities appear for a closed universe, i. e., at $k = 1$. For example, the expansion of a closed universe changes to its contraction, while we see from the Carter-Penrose diagram for a closed universe (see Fig. 2b) that the expansion of the universe cannot change to its contraction, since there is no region T_- for a closed Friedman world. In particular, this is because a time interval will always be found when this diagram will not be valid or, more specifically, the condition $m > m_3$ will be violated. We will give an answer to this question (and to similar questions for other diagrams) at the end of this section.

B. The Case of $m_0 < m < m_3$

This case differs from the previous one only in that the radii ρ_h and ρ_Δ are interchanged. The potential and the Carter-Penrose diagram for an expanding shell for an equation of state with $\alpha = 1/3$ are shown, respectively, in Figs. 2f and 2g ($k = 0, \pm 1$). The Carter-Penrose diagrams for a contracting shell and for other values of α are constructed in much the same way as in the previous case.

C. The Case of $m_2 < m < m_0$

The effective potential in this case shown in Fig. 2h has a region where $U(\rho) > 0$. In this case, the shell bounces, i. e., the contraction and expansion are interchanged, at $U(\rho) = 0$. If the shell begins its motion from the coordinate origin ($\rho(0) = 0$), then the expansion of the shell changes to its contraction and, in the long run, it will contract into a singularity. The Carter-Penrose diagram for a closed world is shown in Fig. 3a. If, alternatively, the shell begins to contract from infinity, then this contraction will change to its expansion and the shell will again expand to infinity. The corresponding Carter-Penrose diagram for a closed world is shown in Fig. 3b.

D. The Case of $m_1 < m < m_2$

For a shell contracting from infinity, the situation will not change compared to the previous case. However, for a shell expanding from the coordinate origin, the situation will change radically. Now, $\sigma_{\text{out}} = +1$. The corresponding graph of the potential and the Carter- Penrose diagram for a closed world are shown in Figs. 3c and 3d.

E. The Case of $m < m_1$

The potential for this case is shown in Fig. 3e. The situation where the shell expands from the coordinate origin will not change compared to the previous case, while the situation where the shell contracts from infinity differs in that the radius ρ_1 will be under the graph of the potential (if it will exist at all by that time). Two alternatives are possible. If the radius ρ_1 is absent at the time when the shell intersects the radius ρ_Δ, then the situation is reduced to the previous case. If, alternatively, the radius ρ_1 exists at the time when the shell intersects the radius ρ_Δ, then $\sigma_{\rm in}$, will change its sign or, more specifically, $\sigma_{\rm in} = -1$. The Carter-Penrose diagram for this alternative is shown in Fig. 3f.

The classification under consideration allows the dynamics of the vacuum shell to be completely described without restricting generality to a short time interval t. Indeed, let the mass m be fixed and the condition $m > m_3$ be satisfied for some short time interval. The parameter m_3 increases with time t and will become larger than m at some time. The condition $m_0 < m < m_3$ will then be satisfied and the vacuum shell will satisfy the corresponding solution for this new inequality depending on whether it intersected other characteristic radii or not. The entire subsequent dynamics of the shell can be traced in a similar way.

The evolution of a contracting vacuum shell can be considered just as the evolution of an expanding one, since the Friedman Eqs. (5) are invariant with respect to the change of sign of the time t to $-t$. Let the vacuum shell begin its motion from the coordinate origin at $t = 0$. The parameter m will then be larger than all of the other mass parameters $m_i = (m_0, m_1, m_2, m_3)$, because $\varepsilon \to \infty$ and $m_i \to 0$ when $t \to 0$.

Let an open or flat universe initially exist inside the vacuum bubble. Nothing will hinder the expansion of the vacuum shell. Depending on the relation between the parameters, several situations can arise. Either the shell will intersect the radius ρ_Δ and then the radius ρ_h or an exchange between the radii will first take place, $\rho_\Delta \lesseqgtr \rho_h$ (since m_3 increases linearly with time, the parameter m_3 will become larger than a given m at some time). If $m > m_0(t \to \infty) = 4/(27\pi S)$, then the shell will just go to infinity. If, alternatively, $m < m_0(t \to \infty) = 4/(27\pi S)$, then the inequality $m < m_0$ will hold after some time (i. e., the potential will intersect the $U = 0$ axis and a bounce point will emerge). However, since the universe inside the bubble is open, the expansion cannot change to contraction, i. e., the vacuum shell can pass only into the region to the right of the graph of the potential (if the shell passed into the region to the left of the potential, then it would bounce at the bounce point and would contract). In the region to the left of the potential, the vacuum shell would continue its expansion, going to infinity. There could also be other special cases during the expansion. For example, $m < m_2(t \to \infty)$, but this case is similar to the previous one. Thus, generally, the Carter-Penrose diagram evolves with time and this evolution is described in different time intervals by the above diagrams.

If, alternatively, a closed universe exists inside the bubble, then there always comes a time when $m < m_0(t \to \infty) = 4/(27\pi S)$, since the expansion should change to contraction. The vacuum shell can then be located only to the left of the potential and the reflection from the bounce point is possible (i. e., the expansion will change to contraction). In the long run, such a shell will contract (collapse) into a singularity.

Qualitatively, the embedding diagrams [34] for vacuum shells in the Friedman-Schwarzschild world are shown in Fig. 4a for open and flat Friedman worlds and in Figs. 4b and 4c for a closed Friedman world (see also [31, 32, 33]). We can see from the Carter-Penrose diagram that semiclosed worlds are formed in almost all cases of shell evolution. This is because the shell moves in the region R_- of the Schwarzschild world, while the regions R_+ and R_- are connected by a tunnel (wormhole).

F. APPROXIMATE SOLUTION

In certain limiting cases, the equation of motion of a vacuum shell in the Friedman-Schwarzschild world can be solved approximately. When the shell contracts from infinity and the effective potential intersects the $U = 0$ axis, the term

$$-\frac{m}{\rho}\left(1-\frac{\varepsilon}{6\pi S^2}\right)-\frac{m^2}{16\pi^2 S^2\rho^4}. \tag{32}$$

can be neglected in the effective potential (13). The equation of motion of the shell (13) will then be significantly simplified and can be reduced to

$$\left(\frac{d\rho}{d\tau}\right)^2 = \phi^2\rho^2 - 1, \tag{33}$$

where we denote $\phi = 2\pi S + \varepsilon/(3S)$. In this case, Eq. (12) for joining the inner Friedman metric and the metric on the shell can be rewritten as

$$\left[1+\left(\frac{d\rho}{d\tau}\right)^2\right]\dot\rho^2 - 2\left(\frac{d\rho}{d\tau}\right)^2 H\rho\dot\rho + \left(\frac{d\rho}{d\tau}\right)^2\left(H^2\rho^2-1\right) = 0, \tag{34}$$

where $H = \dot{a}/a = (8\pi\varepsilon/3)^{1/2}$ is the Hubble constant. From two equations, (33) and (34), we obtain

$$\dot{\rho} = (H\sqrt{\phi^2\rho^2 - 1} \pm |\phi - 4\pi S|)\frac{\sqrt{\phi^2\rho^2 - 1}}{\phi^2\rho}. \quad (35)$$

In this equation, we can already assume that ρ depends only on t. Integrating this equation, we will obtain the function $\rho(t)$ and then can find the function $\tau(t)$ using Eq. (12) at $\rho = aq$:

$$\dot{\tau}^2 = 1 - (\dot{\rho} - H\rho)^2. \quad (36)$$

Finding the inverse function $t = t(\tau)$ from this equation, we will ultimately obtain the function $\rho(\tau)$. For a linear equation of state ($k = 0$) and taking into account the solution of the Friedman equations (6), we have the relation $H = \dot{a}/a = n/t$. Let us find an asymptotic solution to Eq. (35) for $t \to \infty$. In this limit, Eq. (35) can be rewritten as

$$\frac{d\rho}{dt} = \frac{\sqrt{(2\pi S\rho)^2 - 1}}{(2\pi S\rho)^2}\left[\frac{n}{t}\sqrt{(2\pi S\rho)^2 - 1} \pm 2\pi S\right]. \quad (37)$$

Integrating the latter equation at $n \neq 1$ yields

$$\rho = \frac{1}{2\pi S}\sqrt{1 + \frac{(2\pi S)^2[t - Bn(n-1)t^n]^2}{(n-1)^2}}, \quad (38)$$

where B is the constant of integration. Accordingly, at $n = 1$, we obtain

$$\rho = \frac{1}{2\pi S}\sqrt{1 + (2\pi S)^2 t^2 (B + \ln t)^2}. \quad (39)$$

In the limit of $t \to \infty$ under consideration, we ultimately obtain

$$\rho \simeq \begin{cases} [t + B(1-n)nt^n]/(1-n), & n \neq 1; \\ t\ln t, & n = 1. \end{cases} \quad (40)$$

It follows from this solution and Eq. (36) that $d\tau/dt = 0$, i. e., the dependence of t on τ vanishes in the limit under consideration.

The equation of motion of the shell can also be solved in the other limiting case where $t \to 0$. In this limit, the equation of motion of the shell is

$$\frac{d\rho}{dt} = \frac{n}{t}\rho \pm 1. \quad (41)$$

The solution to this equation is

$$\rho \simeq \begin{cases} Ct^n \pm t/(1-n), & n \neq 1; \\ Ct \pm t\ln t, & n = 1, \end{cases} \quad (42)$$

where C is the constant of integration. In this limiting case, there is no dependence of t on τ either.

In a similar way, we can find an approximate solution to the equation of motion of the vacuum shell when it moves while being located to the left of the potential. In this case, terms of the form

$$-\frac{\varepsilon^2\rho^2}{9S^2} - 4\pi^2 S^2\rho^2 - \frac{4\pi}{3}\varepsilon\rho^2. \quad (43)$$

can be neglected in the potential.

The corresponding solutions to the equation of motion of the vacuum shell in the limits $t \to \infty$ and $t \to 0$, are similar in form to (40) and (42).

V. CONCLUSIONS

We considered the dynamics of a thin vacuum shell in the Friedman-Schwarzschild world. The total mass m (Schwarzschild mass) of the shell measured by an observer at spatial infinity is a convenient parameter for the classification of the possible types of its evolution. This mass with the gravitational mass defect includes the total energy of the inner Friedman world and the total energy of the shell with its surface tension energy and its kinetic energy. The classification under consideration allows the dynamics of the vacuum shell to be completely described without restricting generality to a short time interval. The end result of the evolution of the vacuum shells under consideration in the Friedman-Schwarzschild world was shown to be the for motion of black holes and wormholes with baby universes inside in a wide range of initial conditions parameterized by the total initial shell mass. The interior of this world can be a closed, flat, or open Friedman universe. In the same way, more complex configurations, for example, where another bubble inside which a world, other than the Friedman one can be located, is formed within one bubble [13], can be investigated using the method of an effective potential. Such configurations, where the evolution of the inner and outer bubbles is determined by the metrics inside and outside the shell, can be analyzed by the method of an effective potential individually. It should be noted that the method of an effective potential is inapplicable in the situation where the bubbles intersect. In the case of very small bubbles, where the bubble interior is inhomogeneous due to edge effects and the Friedman equations are inapplicable, we go beyond the scope of the formalism under consideration.

[1] D. A. Kirzhnits, Pis'ma Zh. Eksp. Teor. Fiz. 15 (12), 745 (1972) [JETP Lett. 15 (12), 529 (1972)].

[2] D. A. Kirzhnits and A. D. Linde, Phys. Lett. B 42, 471

(1972).
[3] Ya. B. Zel'dovich, I. Yu. Kobzarev, and L. B. Okun', Zh. Eksp. Teor. Fiz. 67 (1), 3 (1974) [Sov. Phys. JETP 40 (1), 1 (1974)].
[4] I. Yu. Kobzarev, L. B. Okun', and M. B. Voloshin, Yad. Fiz. 20, 1229 (1974) [Sov. J. Nucl. Phys. 20, 644 (1975)].
[5] S. Coleman, Phys. Rev. D: Part. Fields 15, 2929 (1977).
[6] C. G. Callan and S. Coleman, Phys. Rev. D: Part. Fields 16, 1762 (1977).
[7] S. Coleman and F. de Luccia, Phys. Rev. D: Part. Fields 21, 3305 (1980).
[8] W. Israel, Nuovo Cimento B 44, 1 (1966).
[9] V. A. Berezin, V. A. Kuzmin, and I. I. Tkachev, Phys. Rev. D: Part. Fields 36, 2919 (1987).
[10] K. Sato, M. Sasaki, H. Kodama, and K. Maeda, Prog. Theor. Phys. 65, 1443 (1981).
[11] K. Sato, M. Sasaki, H. Kodama, et al., Phys. Lett. B 108, 103 (1982).
[12] H. Kodama, M. Sasaki, and K. Sato, Prog. Theor. Phys. 68, 1979 (1982).
[13] H. Kodama, M. Sasaki, K. Sato, et al., Prog. Theor. Phys. 66, 2052 (1981).
[14] V. A. Berezin, V. A. Kuz'min, and I. I. Tkachev, Zh. Eksp. Teor. Fiz. 86 (3), 785 (1984) [Sov. Phys. JETP 59 (3), 459 (1984)].
[15] V. A. Berezin, V. A. Kuz'min, and I. I. Tkachev, Pis'ma Zh. Eksp. Teor. Fiz. 41 (10), 446 (1985) [JETP Lett. 41 (10), 547 (1985)].
[16] V. A. Berezin, V. A. Kuzmin, and I. I. Tkachev, Phys. Lett. B 124, 479 (1983).
[17] V. A. Berezin, V. A. Kuzmin, and I. I. Tkachev, Phys. Lett. B 120, 91 (1983).
[18] V. A. Berezin, V. A. Kuzmin, and I. I. Tkachev, Phys. Lett. B 130, 23 (1983).
[19] J. Ipser and P. Sikivie, Phys. Rev. D: Part. Fields 30, 712 (1984).
[20] A. Aurilia, G. Denardo, F. Legovivni, and E. Spallucci, Phys. Lett. B 147, 258 (1984).
[21] A. Aurilia, G. Denardo, F. Legovivni, and E. Spallucci, Nucl. Phys. B 252, 523 (1985).
[22] A. Aurilia, M. Palmer, and E. Spallucci, Phys. Rev. D: Part. Fields 40, 2511 (1989).
[23] A. Aguirre and M. C. Johnson, Phys. Rev. D: Part. Fields 72, 103525 (2005).
[24] S. K. Blau, E. I. Guendelman, and A. H. Guth, Phys. Rev. D: Part. Fields 35, 1747 (1987).
[25] N. S. Kardashev, I. D. Novikov, and A. A. Shatskiy, Int. J. Mod. Phys. D 16, 909 (2007).
[26] . V. I Dokuchaev and S. V. Chernov, Pis'ma Zh. Eksp. Teor. Fiz. 85 (12), 727 (2007) [JETP Lett. 85 (12), 595 (2007)].
[27] S. V. Chernov and V. I. Dokuchaev, Classical Quantum Gravity 25, 015004 (2008); arXiv:0709.0616v1 [gr-qc]
[28] V. A. Rubakov, Pis'ma Zh. Eksp. Teor. Fiz. 39 (2), 89 (1984) [JETP Lett. 39 (2), 107 (1984)].
[29] V. A. Berezin, V. A. Kuz'min, and I. I. Tkachev, Zh. Eksp. Teor. Fiz. 93 (4), 1159 (1987) [Sov. Phys. JETP 66 (4), 654 (1987)].
[30] M. Ishak and K. Lake, Phys. Rev. D: Part. Fields 65, 044011 (2002).
[31] Ya. B. Zel'dovich, Zh. Eksp. Teor. Fiz. 43, 1037 (1962) [Sov. Phys. JETP 16, 732 (1962)].
[32] V. P. Frolov, M. A. Markov, and V. F. Mukhanov, Phys. Rev. D: Part. Fields 41, 383 (1990).
[33] I. D. Novikov, Pis'ma Zh. Eksp. Teor. Fiz. 3 (5), 223 (1966) [JETP Lett. 3 (5), 142 (1966)].
[34] I. D. Novikov, Vestn. Mosk. Univ., Ser. 3: Fiz., Astron., No. 5, 90 (1962).

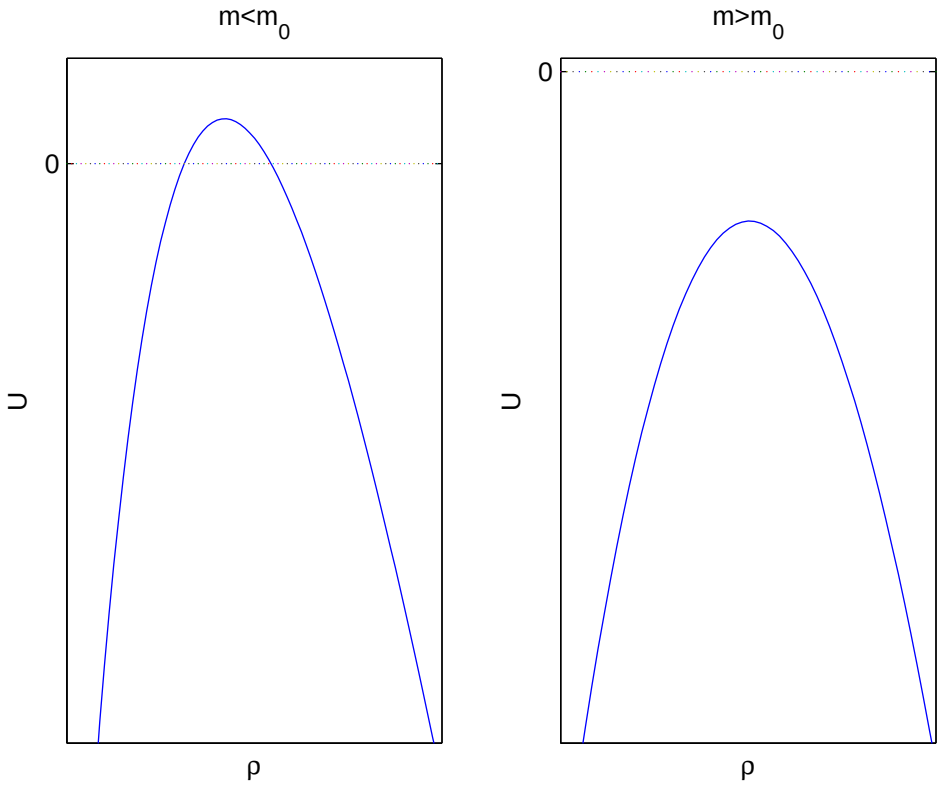

FIG. 1: Effective potential $U(\rho)$ from Eq. (13) as a function of the relation between the total mass m of the shell and the parameter m_0 from Eq. (18): (a) $m < m_0$ and (b) $m > m_0$.

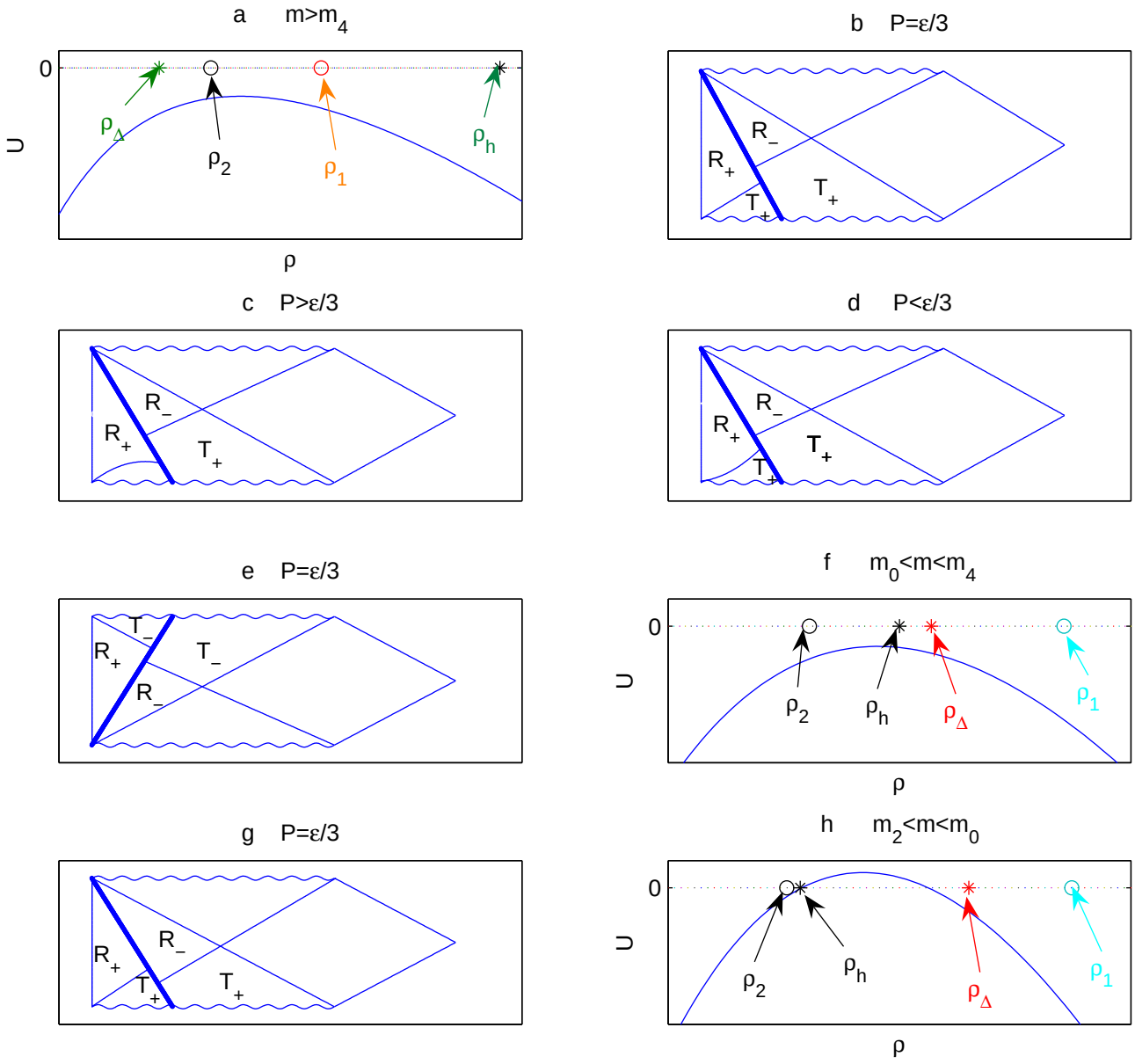

FIG. 2: Effective potentials $U(\rho)$ and Carter-Penrose diagrams for the global geometry of a moving vacuum shell in the Friedman-Schwarzschild world.

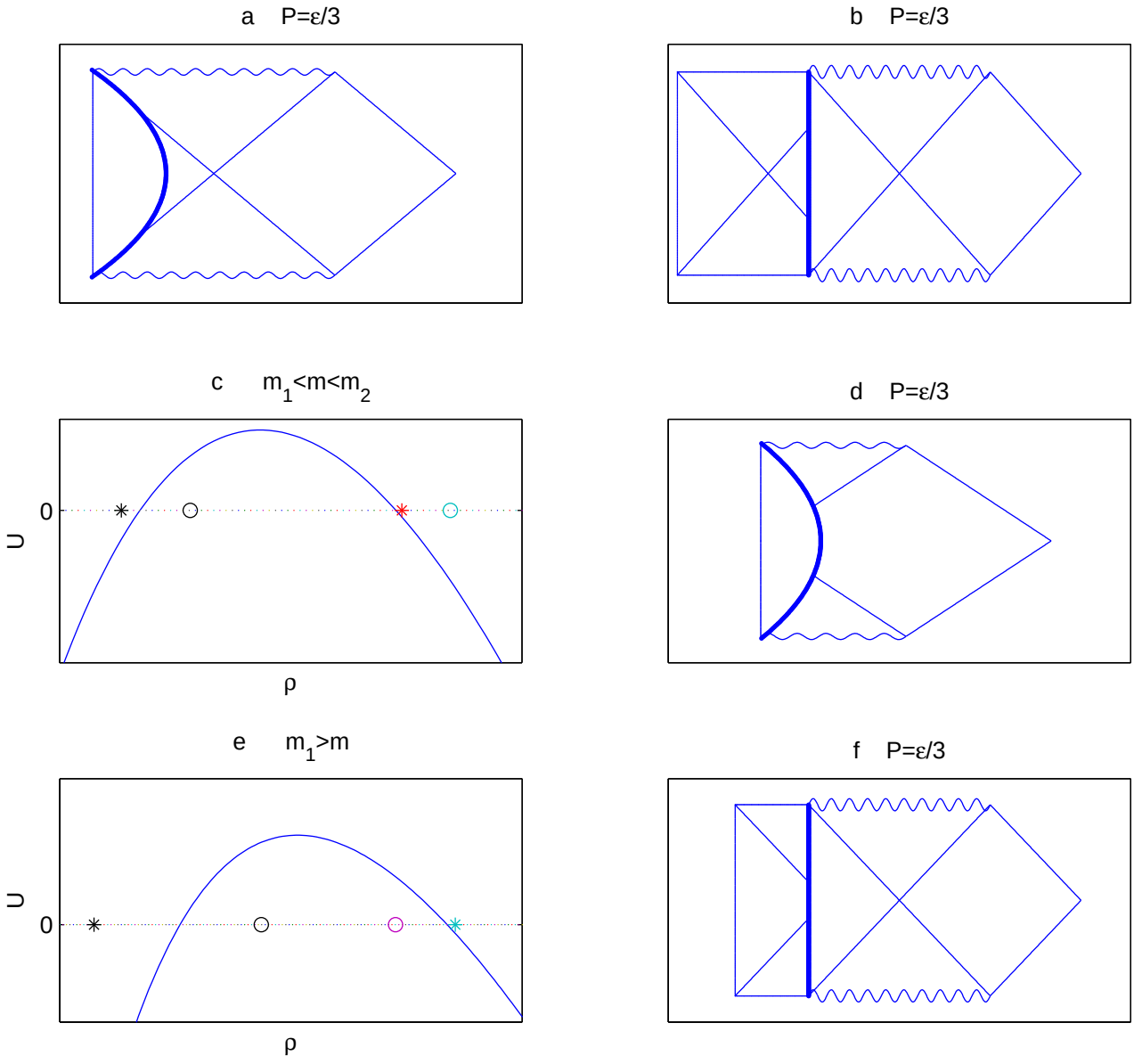

FIG. 3: Effective potentials $U(\rho)$ and Carter-Penrose diagrams for the global geometry of a moving vacuum shell in the Friedman-Schwarzschild world.

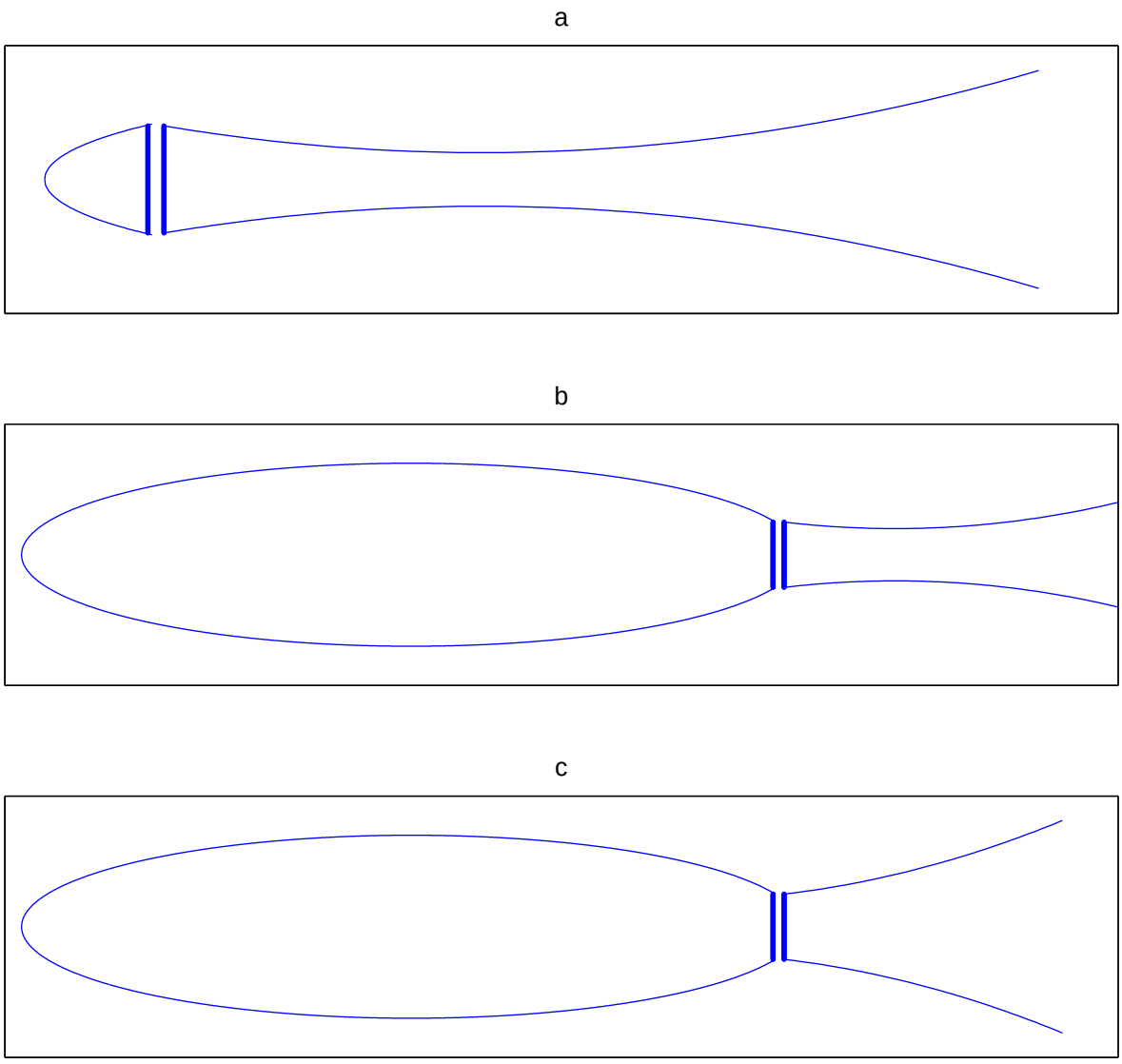

FIG. 4: Embedding diagrams for a shell in the Friedman-Schwarzschild world containing open and flat (a) and closed (b,c) Friedman worlds, respectively.